



GLOBAL JOURNAL OF RESEARCHES IN ENGINEERING: F  
ELECTRICAL AND ELECTRONICS ENGINEERING  
Volume 19 Issue 3 Version 1.0 Year 2019  
Type: Double Blind Peer Reviewed International Research Journal  
Publisher: Global Journals  
Online ISSN: 2249-4596 & Print ISSN: 0975-5861

# Radiated Electromagnetic Interference (Emi) Mechanism of High Power Inverter

By Lingxiang Deng, Pengfei Li, Wanning Bai, Jian Chen, Juhao Fang & Qiangqiang Liu

*Nanjing Normal University*

**Abstract-** In this paper, the generation mechanism of radiated EMI noise in inverter circuit is analyzed. On the basis of analyzing the equivalent model of common mode and differential mode radiated EMI noise, the radiated EMI noise is separated by common mode and differential mode by using the fast Fourier transform principle. The effectiveness of the radiated EMI noise separation method is verified by experiments.

**Keywords:** *high-power inverter, electromagnetic interference (EMI), radiation emission (RE), common mode radiation, differential mode radiation, radiated EMI noise separation method.*

**GJRE-F Classification:** FOR Code: 040401



*Strictly as per the compliance and regulations of:*



© 2019. Lingxiang Deng, Pengfei Li, Wanning Bai, Jian Chen, Juhao Fang & Qiangqiang Liu. This is a research/review paper, distributed under the terms of the Creative Commons Attribution-Noncommercial 3.0 Unported License (<http://creativecommons.org/licenses/by-nc/3.0/>), permitting all non commercial use, distribution, and reproduction in any medium, provided the original work is properly cited.

# Radiated Electromagnetic Interference (EMI) Mechanism of High Power Inverter

Lingxiang Deng <sup>α</sup>, Pengfei Li <sup>σ</sup>, Wanning Bai <sup>ρ</sup>, Jian Chen <sup>ω</sup>, Juhao Fang <sup>¥</sup> & Qiangqiang Liu <sup>§</sup>

**Abstract-** In this paper, the generation mechanism of radiated EMI noise in inverter circuit is analyzed. On the basis of analyzing the equivalent model of common mode and differential mode radiated EMI noise, the radiated EMI noise is separated by common mode and differential mode by using the fast Fourier transform principle. The effectiveness of the radiated EMI noise separation method is verified by experiments.

**Keywords:** high-power inverter, electromagnetic interference(EMI), radiation emission (RE), commonmode radiation, differential mode radiation, radiated EMI noise separation method.

## I. INTRODUCTION

With the rapid development of power electronics, inverter systems with highpower inverter power supply as the core are more and more widely used in large-scale power equipment[1-5]. However, the increase of power density leads to the increasingly complex electromagnetic environment inside the inverter system[6-10]. The resulting radiated electromagnetic interference can cause equipment failure and pose a potential hazard to the safe and reliable operation of itself and other surrounding equipment[11-12]. Therefore, it is necessary to study the mechanism of radiated electromagnetic interference of high-power inverters [13].

The radiated EMI noise is generated by the inverter circuit and the loop equivalent antenna [14-15]. The device under tested (EUT) is placed at the coordinates , the measured point is at x, and the length of the EUT equivalent radiating antenna is l, then the equivalent radiated antenna is measured. The distance between points can be expressed as

$$r=R-n \cdot x' \quad (1)$$

Where R is the distance between the origin and the point to be measured, and n is the unit vector in the R direction. The wavelength corresponding to the radiation noise is

$$\lambda=\frac{c}{f} \quad (2)$$

Author <sup>α</sup>: Jiangsu Institute of Metrology, Nanjing Jiangsu China. e-mail: 448221017@qq.com

Author <sup>σ ρ ω ¥ §</sup>: Nanjing Normal University, Nanjing, Jiangsu. China. e-mail: 1730312514@qq.com

In the above formula, c is  $3 \times 10^8$  m/s,  $\lambda$  is the wavelength corresponding to the radiation noise, and f is the frequency of the radiated EMI noise caused by the EUT.

Because the size of the high-power inverter power cabinet is 800mm  $\times$  500mm  $\times$  1500mm (width  $\times$  depth  $\times$  height), and according to the simulation calculation f is about 80kHz,  $\lambda$  is 3750m, the transmission control cabinet The size is obviously less than 1/10 of the wavelength of the radiation. It can be considered that the above radiation test condition is a small size characteristic, and the current density in the equivalent antenna is J, which can be derived.

$$A(x)=\frac{\mu_0}{4\pi} \int \frac{J(x')e^{jk(R-n \cdot x')}}{R-n \cdot x'} dV' \quad (3)$$

A is a retarded potential, and k is the wave vector. The  $-n \cdot x'$  term in the denominator of (3) can be omitted, and  $e^{-jkn \cdot x'}$  will be expanded by  $kn \cdot x'$ .

$$A(x)=\frac{\mu_0 e^{j k R}}{4\pi} \int J(x')(1-jkn \cdot x'+\dots) dV' \quad (4)$$

The first two parts of equation (4) represent electric dipole common mode radiation and magnetic dipole differential mode radiation, respectively.

## II. RADIATED EMI NOISE MODELING

### a) Common mode EMI noise model

As shown in Fig. 1, for common mode radiation, it can be equivalent to an electric dipole antenna, and the delay potential is the first part of equation (4).

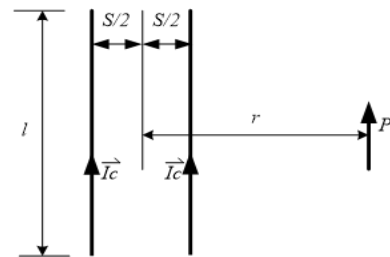


Fig. 1: Common mode noise equivalent model

$$A(x)=\frac{\mu_0 e^{j k e R}}{4\pi R} \int J(x') dV' \quad (5)$$

In the electric dipole antenna, there are ni particles with a velocity of vi and a charge of qi per unit volume. then

$$J = \sum_i n_i q_i v_i \tag{6}$$

$$P = \sum q_i v_i \tag{7}$$

Where  $\dot{p}$  is the first derivative of the electric dipole moment versus time.

Therefore, the magnetic field strength, electric field strength, energy flow density and radiation power of the electric dipole can be derived.

$$B_{CM} = \frac{1}{4\pi\epsilon_0 c^3 R} \left| \dot{p} \right| e^{jkR} \sin \theta e_\phi$$

$$E_{CM} = \frac{1}{4\pi\epsilon_0 c^2 R} \left| \dot{p} \right| e^{jkR} \sin \theta e_\phi$$

$$S_{CM} = \frac{1}{32\pi^2 \epsilon_0 c^3 R^2} \left| \dot{p} \right|^2 \sin^2 \theta_n$$

$$P_{CM} = \frac{1}{4\pi\epsilon_0} \frac{\left| \dot{p} \right|^2}{3c^3}$$
(8)

According to equation (8) and Maxwell's equations, the calculated common mode radiated noise generated by the electric dipole at far field r is

$$E_{CM} = 12.6 \times 10^{-7} \frac{f I_{CM}}{r} \tag{9}$$

$I_{CM}$  is the common mode current in the electric dipole, l is the length of the electric dipole antenna, and r is the distance between the measured point and the center of the electric dipole. Therefore, equations (8), (9), and (1) can describe the principle and model of electric dipole common mode radiation noise.

b) Differential mode EMI noise model

As shown in Fig. 2, for differential mode radiation, it can be equivalent to a magnetic dipole antenna, which delays the second part of the potential size formula (4).

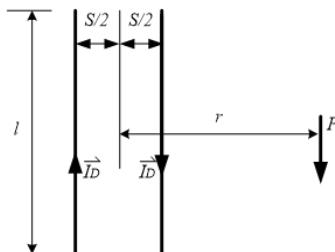


Fig. 2: Differential mode noise model

$$A(x) = \frac{-jk\mu_0 e^{jkR}}{4\pi R} \int J(x')(n \cdot x') dV' \tag{10}$$

The magnetic field strength, electric field strength, energy flow density and radiant power of the magnetic dipole antenna are

$$B_{DM} = \nabla \times A = \frac{\mu_0 e^{jkR}}{4\pi c^2 R} (m \times n) \times n$$

$$E_{DM} = cB \times A = -\frac{\mu_0 e^{jkR}}{4\pi c R} (m \times n)$$

$$S_{DM} = \frac{\mu_0 \omega^4 |m|^2}{32\pi^2 c^3 R^2} \sin^2 \theta_n$$

$$P_{DM} = \frac{\mu_0 \omega^4 |m|^2}{12\pi c^3}$$
(11)

From the equation (11) and the Maxwell equations, considering the grounding total reflection, the differential mode radiated noise of the magnetic dipole antenna at the far field r

$$E_{DM} = 2.632 \times 10^{-14} \frac{f^2 A I_{DM}}{r} \tag{12}$$

$I_{DM}$  is the differential mode current in the magnetic dipole, A is the area of the magnetic dipole antenna, and r is the distance between the measured point and the center of the electric dipole. Therefore, equations (11), (12), and Fig. 2 can describe the principle and model of magnetic dipole differential mode radiated noise.

### III. RADIATED EMI NOISE SEPARATION METHOD

The second section of the above section establishes the electric dipole common mode radiation and the magnetic dipole differential mode radiation acoustic model, The nature of the radiated noise is analyzed when the radiated noise is suppressed. Therefore, this section designs a radiated noise separation method based on short-time fast Fourier transform and independent component analysis for common mode noise and differential mode noise electromagnetic characteristics.

Using the field probe to receive the radiated noise  $Z_1(t), Z_2(t), \dots, Z_N(t)$  of the N sets of EUTs, perform short-time fast Fourier transform on the acquired time domain signal  $Z(t)$ .

$$SIFT_z(t, f) = \int_{-\infty}^{\infty} [z(t') \gamma'(t-t')] e^{-2\pi f t'} dt' \tag{13}$$

Where  $\gamma(t)$  is the time window and \* indicates its conjugate complex number. The time-rate energy distribution (instantaneous power spectral density) of the STFT is the square of the STFT(t, f) modulus.

$$SPEC(t, f) = |STFT(t, f)|^2 \tag{14}$$

The digital representation of the STFT can be derived from the equations (13) and (14).

$$STFT(n, k) = \sum_{i=0}^{N-1} [x_i \gamma^*(i-n)] \exp(-j \frac{2\pi ki}{N}) \tag{15}$$

$$SPEC(n, k) = |STFT(t, f)|^2 \tag{16}$$

Where N represents the amount of FFT data, and n and k represent the discrete time number of the time-frequency and the number of frequency grids, respectively. In the application, the fast algorithm of equation (16) is generally implemented by Fourier transform.

Through independent component analysis, the characteristics of the received noise signal are extracted, and then the short-time fast Fourier transform is used to convert the separated time domain noise signal into the frequency domain, and compared with the circuit under test, the source of the radiated electromagnetic interference noise is located. the specific method implementation steps are as follows:

- a) Using a high-speed oscilloscope to perform near field testing on the EUT, extracting N sets of mixed radiated noise time domain signals Z(t);
- b) Perform independent component analysis on the noise signal Z(t) and separate the mixed signal into N independent radiated noise signal sources Z1(t), Z2(t), ... ZN(t) as alternative sources of radiated noise ;
- b) The independent noise sources Z1(t), Z2(t), ... ZN(t) are obtained by short-time fast Fourier time frequency analysis, and the signal characteristics of the noise source are extracted;
- c) Compare the signal characteristics obtained after analysis with the circuit under test to find out the components that cause the radiation to exceed the standard.

#### IV. RADIATED EMI NOISE SEPARATION EXPERIMENT

This verification experiment uses a multi track high speed oscilloscope to measure the radiated noise time domain signal of the EUT through a mufti channel test port with a near-field magnetic field probe, as shown in Fig. 3.

The near-field magnetic field probe uses Rhode & Schwarz's near-field probe set HZ-11, which has a

frequency detection range of 10 kHz to 2 GHz as shown in Fig. 3. The multi track high-speed oscilloscope uses the Tektronix DPO5204 model with a bandwidth of up to 2 GHz and four test channels with a sampling rate range of 5 GS/s - 10 GS/s. In the experiment, the sampling rate of the oscilloscope DPO5204 is set to 1GS/s, and the EUT radiated noise time domain signal can be acquired.

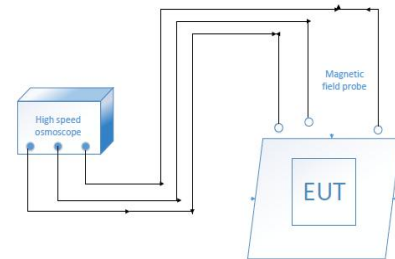


Fig. 3: Experimental arrangement



Fig. 4: Experimental measurement

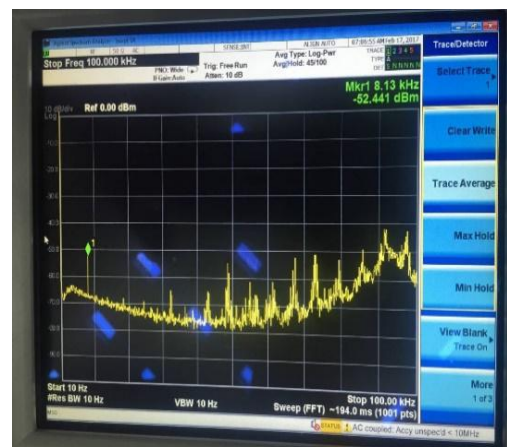
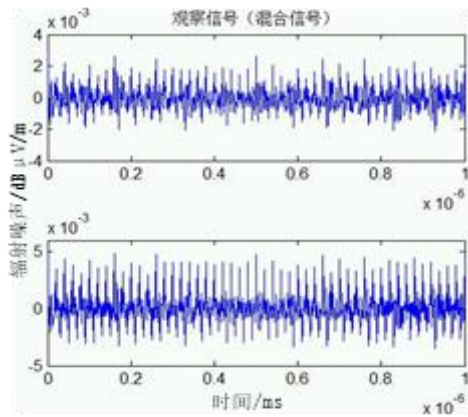


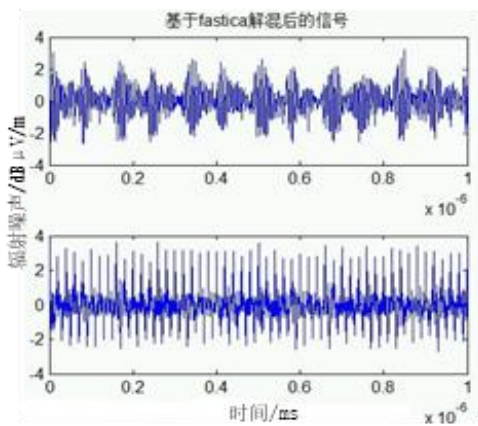
Fig. 5: Inverter power supply radiation noise near field test results

Firstly, the radiated noise mixed time domain signal of the high-power inverter power supply is collected. The measured near-field noise test result is shown in Fig. 6. After the noise signal is introduced into MATLAB, the time domain characteristics of the noise

signal are shown in Fig. 6 (a). Perform independent component analysis, as shown in Fig. 6(b). There are two independent noise signals Z1(t) and Z2(t). The time-frequency analysis is shown in Fig. 7. As can be seen from Fig. 7(a), the data with the strongest energy in the noise is extracted as shown in Table 1. The average value of the data in the table is about 240 MHz. It can be seen that the noise is strongest around 240 MHz, and the internal inverse is observed. The variable circuit found that the crystal frequency of the control board is 30MHz, and 240MHz is its frequency multiplication, so the noise is the radiation noise generated by the 30MHz crystal oscillator. As seen in Fig. 7(b), the noise is the strongest at 300KHz, and the noise signal data at the strongest energy is extracted as shown in Table 2. The average value is 299.85KHz, which is compared with the internal inverter circuit. The power master chip operates at a frequency of 100 kHz and 300 kHz as its frequency multiplier. Therefore, the noise after the separation is the radiation noise of the 100 KHz master chip. It can be seen that the radiation noise of the device is mainly generated by the 30M crystal oscillator and the 100KHz main control chip.



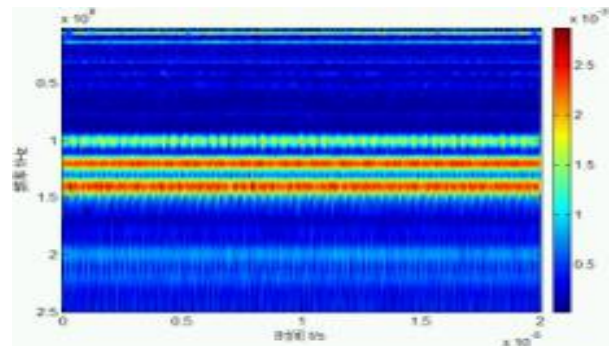
(a) Mixed time domain signals



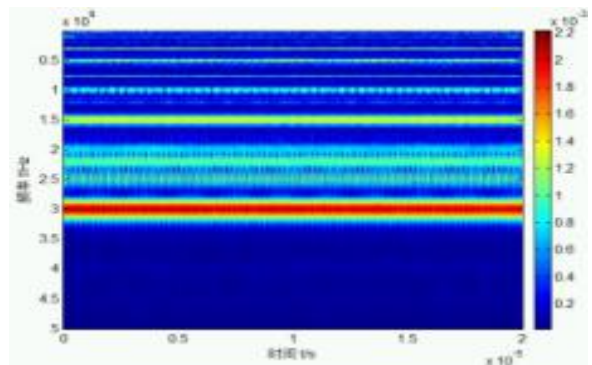
(b) Time domain signal after separation

Fig. 6: Time domain signal before and after the separation of radiated noise of inverter power supply

Comparing the separated noise signals can judge the strength of the two signals. Comparing Tables 1 and 2, the energy intensity of the 30MHz noise signal is stronger in the noise signals after separation between the two groups. Therefore, the 30MHz noise signal is the main cause of the radiation noise exceeding the standard of the device under test. From the above analysis, the 30MHz crystal oscillator is large. The main reason for the excessive radiation noise of the power inverter power supply cabinet provides a theoretical basis for the suppression of subsequent radiation noise.



(a) Time-frequency analysis results of Z1(t)



(b) Time-frequency analysis results of Z2(t)

Fig. 7: Time-frequency analysis results of radiation noise of high-power inverter power supply

Table 1: Time-frequency analysis data of the radiated noise Z1(t) after separation

time*10 $\mu$ s	frequency/MHz	Energy intensity *10 $^{-3}$
2.475	239.4	2.484
5.723	239.4	2.343
9.446	239.7	2.513
13.21	240.0	2.311
15.74	239.4	2.64
18.59	240.1	2.46

**Table 2:** Time-frequency analysis data of the radiated noise Z2(t) after separation

time*10 $\mu$ s	frequency/MHz	Energy intensity *10 $^{-3}$
1.525	299.5	1.147
2.059	299.5	1.017
6.99	300.0	1.029
13.64	300.3	1.032
15.78	299.7	1.136
18.28	300.1	1.022

## V. CONCLUSION

In short, the mechanism of radiated EMI noise generation in inverter circuit has been analyzed, and the method of common mode and differential mode separation of radiated EMI noise by using the principle of fast Fourier transform is proposed. The effectiveness of the method of radiating EMI noise separation is verified by experiments. Sex. As a result, a better solution to EMI noise can be proposed.

## REFERENCES RÉFÉRENCES REFERENCIAS

1. K. C. Su and J. Li, "Research on Eliminating High-order Harmonics of Inverter Output Voltage", Journal of South China University of Technology(Natural Science Edition),vol.19, Issue:1, pp.65-72,1991.
2. GB T 6113-2008. Specification and Measurement Methods for Radio Disturbance and Immunity Measurement Equipment. 2008.
3. GB T 17626-2006. Electromagnetic Compatibility Test Methods and Testing Techniques. 2006.
4. Y. S. Yuan and G. L. Qian, "Modeling of Power MOSFETs for Conducting EMI ", Journal of Zhejiang University (Engineering Science), vol.37, Issue:2, pp.198-201,2003.
5. E. Hertz, "Thermal and EMI Modeling and Analysis of a Boost PFC Circuit Designed Using a Genetic-Based Optimization ", Virginia Tech, 2001.
6. J. P. He, W. Chen and J. G. Jiang, "Research on Common Mode Conducted Interference Model of Switching Power Supply", Proceedings of the CSEE, vol.25, Issue:8, pp.50-55,2005.
7. J. P. He, W. Chen and J. G. Jiang, "Analysis of the effect of stray magnetic field on conductionCSEE,vol.25, Issue:14, pp.151-157,2005.
8. Y. B. Zhou, "Research on Common Mode EMI Analysis and Active Suppression Technology for Single-Phase Inverter", Huazhong University of Science and Technology, 2006.
9. interference emission in power", factor correction circuit. Proceedings of the
10. K. Zhang, H. S. Fang and Y. B. Zhou, et al. "Research on common mode equivalent circuit of single-phase full-bridge inverter", Transactions of China Electrotechnical Society, vol.22, Issue:2, pp.51-56,2007.
11. K. Zhang, Z. Y. Liu and X. J. Qi, et al. "Full- Bridge Circuit Common Mode Suppression Technology Based on Drive Pulse Self- Calibration", Proceedings of the CSEE, vol.27, Issue:13, pp. 58-63,2007.
12. Z. M. Qian and W. J. Cheng, "Electromagnetic Interference Design and Interference Suppression Technology for Power Electronic Systems ", Zhejiang University Press, pp.78- 96,2000.
13. G. L. Qian, Z. Y. Lu and X. N. He , "EMC Design of High Power Converters ", Proceedings of the 14th National Conference on Power Technology, pp. 487-490,2001.
14. Y. B. Peng and Y. Q. Tang, "Research on Electromagnetic Compatibility of Transmission System", Electric Drive, vol.16, Issue:9, pp.98-100,2007.
15. X. Y. Zhang, "Research on Electromagnetic Interference and Suppression of Electric Vehicle Motor Inverter System ", Beijing Institute of Technology, 2016.
16. A. Sarikhani,M. Barzegaran and O. A. Mohammed, "Optimum Equivalent Models of Multi-source Systems for the Study of Electromagnetic Signatures and Radiated Emissions From Electric Drives", IEEE Transactions on Magnetics Mag,vol.48, Issue:2, pp.1011-1014,2012.